International Journal of Advanced Engineering Research and Science (IJAERS)
Peer-Reviewed Journal
ISSN: 2349-6495(P) | 2456-1908(O)
Vol-11, Issue-5; May, 2024
Journal Home Page Available: https://ijaers.com/
Article DOI: https://dx.doi.org/10.22161/ijaers.115.1

Alternative Algorithms for Time Series Water Wave Modeling

Syawaluddin Hutahaean

Ocean Engineering Program, Faculty of Civil and Environmental Engineering,-Bandung Institute of Technology (ITB), Bandung 40132, Indonesia
syawalf1@yahoo.co.id

Received: 07 Mar 2024,

Receive in revised form: 21 Apr 2024,

Accepted: 03 May 2024,

Available online: 11 May 2024

***Keywords*— calculation algorithm, conservation of energy.**

***Abstract*—** *This research builds upon Hutahaean (2024a), focusing on time series water wave modeling, with substantial portions of this article derived from that prior study. Modifications were made to the calculation algorithm; specifically, vertical water particle velocity is now computed using the continuity equation, and water surface elevation is determined through kinematic free surface boundary conditions. While this revised algorithm enables the model to simulate wave breaking, it results in an excessively high breaker height and struggles to accurately simulate wave conditions post-breaking, particularly at large wave heights. To address these challenges, the kinetic energy conservation equation was integrated into the model. This addition facilitated the creation of a water surface elevation equation through the superposition of kinematic free surface boundary conditions and the kinetic energy conservation equation. This integration yields an equation that maintains a balance between changes in potential energy and changes in kinetic energy, enhancing the model's capability to simulate both the shoaling-breaking process and subsequent wave conditions in shallow waters more effectively.*

I. INTRODUCTION

Time series water wave modeling continues to evolve, particularly due to challenges in accurately modeling complex phenomena such as wave diffraction at breakwater gaps. Traditional methods based on velocity potential theory often fall short in these areas. A more robust approach is the use of the Boussinesq equation, which has been significantly developed by researchers such as Boussinesq, J. (1871), Dingermans, M.W. (1997), Hamm, L., Madsen, P.A., Peregrine, D.H. (1993), Johnson, R.S. (1997), Kirby, J.T. (2003), and Peregrine, D.H. (1967, 1972), among others.

The conventional time series water wave model primarily comprises two equations: the water surface elevation equation and the horizontal water particle velocity equation. The former is formulated by integrating the continuity equation—taking into account both water depth and vertical surface particle velocity—and applying the Free Surface Boundary Condition. This model is adept at representing shoaling but falls short in simulating wave breaking and post-breaking conditions in shallow waters. While some advancements have been made, as demonstrated by Hutahaean, S. Achiari H. (2017) and Hutahaean S. (2019), the ability to reliably simulate post-breaking conditions remains inconsistent, with some datasets accurately modeled and others not.

Building on this knowledge, recent research by Hutahaean (2024b) has made significant strides. Utilizing velocity potential theory, this study identified that breaking characteristics are prominent in the Kinematic Free Surface Boundary Condition. Leveraging this insight, a new time series water wave model has been developed, incorporating the Kinematic Free Surface Boundary Condition for calculating water surface elevations. This model also utilizes the continuity equation to determine vertical water particle velocities.

The current model successfully simulates shoaling and breaking but tends to overestimate the height of breaking waves and fails to accurately model wave behavior as it progresses into very shallow waters. One significant limitation identified is within the Kinematic Free Surface Boundary Condition, which accounts for changes in potential energy due to variations in water surface elevation without a corresponding adjustment for kinetic energy. This oversight results in an energy imbalance, as there's no accounted source of energy to facilitate the observed changes in potential energy.

To rectify this issue, the model has been refined by integrating the Kinematic Free Surface Boundary Condition with a conservation of kinetic energy equation. This integration ensures a balanced accounting of energy changes, which enhances the accuracy of the water surface elevation predictions.

Additionally, modifications have been made to the Euler momentum conservation equation, as detailed in Hutahaean (2024a). The updated Euler Momentum Conservation Equation now strictly enforces that horizontal velocity changes occur only on the horizontal axis and vertical velocity changes only on the vertical axis.

With these critical modifications, the enhanced time series model now more accurately simulates wave breaking, effectively extending its predictive capabilities to shallow waters near the coast.

II. WEIGHTED TAYLOR SERIES

In this paper, we adopt the $x-z$ coordinate system, where the x -axis represents the horizontal axis and the z -axis denotes the vertical axis.

A weighted Taylor series is a truncated Taylor series limited to first-order terms, with the influence of higher-order terms encapsulated in coefficients known as weighting coefficients.

For a function of two variables $f = f(x\ ,t)$

$$f(x+\delta x, t+\delta t) = f(x,t) + \gamma_{t,2}\delta t\frac{\partial f}{\partial t} + \gamma_x \delta x\frac{\partial f}{\partial x} \quad \ldots.(1)$$

$\gamma_{t,2}$ and γ_x are weighting coefficients.

For function $f = f(x,z,t)$ the weighted Taylor series is

$$f(x+\delta x, z+\delta z, t+\delta t) = f(x,z,t) + \gamma_{t,3}\delta t\frac{\partial f}{\partial t} + \gamma_x \delta x\frac{\partial f}{\partial x} + \gamma_z \delta z\frac{\partial f}{\partial z} \quad \ldots(2)$$

$\gamma_{t,3}$, γ_x and γ_z are weighting coeffcients. There is no difference between γ_x in $f(x,t)$ and γ_x in $f(x,z,t)$. The basic values of these weighting coefficients are, $\gamma_{t,2} = 2$, $\gamma_{t,3} = 3$, $\gamma_x = 1$ and $\gamma_z = 1$.

The updated weighting coefficient values are presented in Table (1), wherein these coefficients are dependent on the optimization coefficient ε . A larger ε corresponds to a greater influence of higher-order Taylor series terms. The methodology for computing these weighting coefficients is detailed in Hutahaean (2023). However, the precision of the weighting coefficients listed in Table (1) surpasses that of Hutahaean (2023).

In this particular time series model, the selection of weighting coefficients hinges on the wave amplitude. Specifically, a higher wave amplitude corresponds to a larger ε , falling within the range of $0.15 \leq \varepsilon \leq 0.35$.

Table (1) Weighting coefficients.

ε	$\gamma_{t,2}$	$\gamma_{t,3}$	γ_x	γ_z
0.010	1.999797	3.004905	0.998792	1.011458
0.012	1.999707	3.007157	0.998257	1.016713
0.014	1.999600	3.009870	0.997625	1.023049
0.016	1.999477	3.013062	0.996894	1.030512
0.018	1.999336	3.016751	0.996064	1.039152
0.020	1.999178	3.020955	0.995135	1.049022
0.022	1.999002	3.025692	0.994107	1.060178
0.024	1.998809	3.030982	0.992979	1.072679
0.026	1.998599	3.036843	0.991751	1.086589
0.028	1.998370	3.043296	0.990422	1.101976
0.030	1.998124	3.050358	0.988994	1.118910
0.032	1.997859	3.058049	0.987464	1.137468
0.034	1.997576	3.066390	0.985834	1.157729
0.036	1.997275	3.075398	0.984104	1.179778
0.038	1.996954	3.085094	0.982272	1.203703
0.040	1.996615	3.095495	0.980339	1.229598

With the weighted Taylor series, the kinematic free surface boundary condition becomes,

$$w_\eta = \gamma_{t,2}\frac{\partial \eta}{\partial t} + \gamma_x u_\eta \frac{\partial \eta}{\partial x} \quad \ldots\ldots\ldots\ldots..(3)$$

w_η = vertical surface water particle velocity

u_η = horizontal surface water particle velocity

$\eta(x,t)$, water surface elevation equation.

Meanwhile, the total acceleration of horizontal and vertical water particles is,

$$\frac{Du}{dt} = \gamma_{t,3}\frac{\partial u}{\partial t} + \frac{\gamma_x}{2}\frac{\partial uu}{\partial x} + \gamma_z w\frac{\partial u}{\partial z}$$

$$\frac{Dw}{dt} = \gamma_{t,3}\frac{\partial w}{\partial t} + \gamma_x u\frac{\partial w}{\partial x} + \frac{\gamma_z}{2}\frac{\partial ww}{\partial z}$$

III. DEPTH AVERAGE VELOCITY

The model is formulated using depth average velocity as its variable, where according to Dean (1991), the horizontal depth average velocity is,

$U = \frac{1}{\beta_u D}\int_{-h}^{\eta} u\ dz$ .....(4)

U = horizontal depth average velocity

β_u = the horizontal velocity integration coefficient

$D = h + \eta$

D = total water depth

h = water depth towards still water level (Fig. 1)

η = surface water level towards still water level (Fig.1)

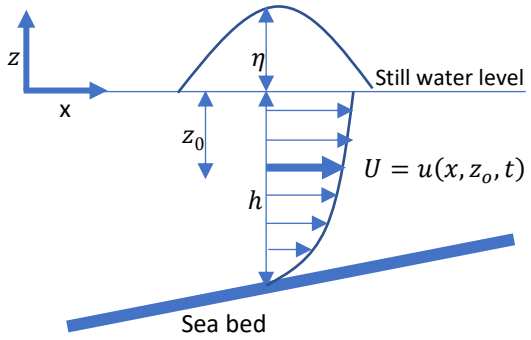

Fig (1). Depth average velocity concept

Equation (4) was initially formulated to model very long waves, such as tidal waves, using a horizontal velocity integration coefficient $\beta_u = 1$. In this study, the integration coefficient is calculated by defining the depth-averaged velocity as the velocity at a depth $z = z_0$ below the still water level. Here, z_0 is negative, as shown in Figure 1. Consequently, z_0 is defined in terms of the water depth h, specifically $z_0 = -\xi h$, where $0 < \xi < 1$.

The velocity potential equation solution of Laplace equation is

$\phi(x,z,t) = G(\cos kx + \sin kx)\cosh k(h+z)\sin \sigma t$

G is wave constant

k is wave number

σ is angular frequency, $\sigma = \frac{2\pi}{T}$

T is wave period.

a. Coefficients of Integration β_u and β_w

Horizontal water particle velocity from velocity potential is

$$u(x,z,t) = -\frac{\partial \phi}{\partial x} = -Gk(-\sin kx + \cos kx)\cosh k(h + z)\sin \sigma t$$

Vertical water particle velocity is

$$w(x,z,t) = -\frac{\partial \phi}{\partial z} = -Gk(\cos kx + \sin kx)\sinh k(h + z)\sin \sigma t$$

Based on the definition of the horizontal depth average velocity,

$$U = u(x,-\xi h,t) = -Gk(-\sin kx + \cos kx)\cosh kh(1-\xi)\sin \sigma t$$

Thus,

$$\frac{u}{U} = \frac{\cosh k(h+z)}{\cosh kh\ (1-\xi)}$$

Equation (4) is written into the equation for β_u,

$$\beta_u = \frac{1}{UD}\int_{-h}^{\eta} u\ dz$$

$$\beta_u = \frac{1}{D\cosh kh(1-\xi)}\int_{-h}^{\eta}\cosh k(h+z)\ dz$$

$$\beta_u = \frac{\sinh k(h+\eta)}{kD\cosh kh(1-\xi)}$$

$$\beta_u = \frac{\sinh kD}{kD\cosh kh(1-\xi)}$$

In deep water, $kD \approx kh = \theta\pi$, θ is referred to as the deep water coefficient where $\tanh \theta\pi = 1$, and $\theta = 1.70$ is used in this research

$\beta_u = \frac{\sinh \theta\pi}{\theta\pi\cosh \theta\pi(1-\xi)}$ .....(5)

Although this equation is formulated in deep water, it also applies to shallow water, given the law of conservation of wave number (Hutahaean (2024b)) , where

$$\frac{\partial k(h+z)}{\partial x} = 0$$

Thereby $k(h+z)$ is constant, unchanged against changes in water depth, as well as $k(h+\eta)$ is constant .

The integration coefficient of the vertical depth average velocity β_w , is formulated in the same way,

$$\beta_w = \frac{1}{DW}\int_{-h}^{\eta} w\ dz$$

$$\beta_w = \frac{1}{D\sinh kh(1-\xi)}\int_{-h}^{\eta}\sinh k(h+z)\ dz$$

$$\beta_w = \frac{\cosh kD - 1}{kD\sinh kh(1-\xi)}$$

$\beta_w = \frac{\cosh \theta\pi - 1}{\theta\pi\sinh \theta\pi(1-\xi)}$ .....(6)

b. Transformation coefficients

In the derivation of equations for water surface elevation and water particle velocity, variables for surface water particle velocities, namely horizontal velocity u_η and vertical velocity w_η, are introduced. To apply these equations more broadly, it is necessary to transform these surface velocities into depth-averaged velocities.

Using the definition of the depth average velocity,

$$\alpha_{u\eta} = \frac{u_\eta}{U} = \frac{\cosh k(h+\eta)}{\cosh kh(1-\xi)} = \frac{\cosh \theta\pi}{\cosh \theta\pi(1-\xi)}$$

Or

$u_\eta = \alpha_{u\eta} U$

Where the transformation coefficient $\alpha_{u\eta}$ is,

$$\alpha_{u\eta} = \frac{\cosh \theta\pi}{\cosh \theta\pi(1-\xi)} \quad \text{.....(7)}$$

Since $u_\eta u_\eta$ and $u_\eta u_\eta u_\eta$ is derived from u_η Thus its distribution over space and time is the same as u_η. Therefore, its transformation coefficient is the same as the transformation coefficient of u_η.

$u_\eta u_\eta = \alpha_{u\eta} UU$

$u_\eta u_\eta u_\eta = \alpha_{u\eta} UUU$

The vertical velocity transformation coefficient is

$$\alpha_{w\eta} = \frac{w_\eta}{W} = \frac{\sinh \theta\pi}{\sinh \theta\pi(1-\xi)} \quad \text{.....(8)}$$

A relationship is obtained,

$w_\eta = \alpha_{w\eta} W$

$w_\eta w_\eta = \alpha_{w\eta} WW$

$w_\eta w_\eta w_\eta = \alpha_{w\eta} WWW$

In this study $\theta = 1.70$, $\xi = 0.32$, are used, with

$\beta_u = 1.033$, $\alpha_{u\eta} = 5.52$, $\alpha_{w\eta} = 5.53$

The effect of θ value is that the larger the θ value, the deeper the breaker depth and vice versa, the smaller the θ value, the smaller the breaker depth, but has no effect on the breaker height value.

IV. THE CONSERVATION EQUATIONS

4.1.Weighted continuity equation.

The continuity equation is formulated using the weighted Taylor series and by working on the conservation of mass principle,,

$$\gamma_x \frac{\partial u}{\partial x} + \gamma_z \frac{\partial w}{\partial z} = 0 \quad \text{.....(9)}$$

This equation is formulated under the condition that horizontal particle velocity only changed on the horizontal axis, as well as vertical particle velocity only changes on the vertical axis.

4.2. Kinetic Energy Conservation Equation

The kinetic energy conservation equation is formulated by reviewing the inflow and outflow of kinetic energy in a control volume. In the moving fluid mass contained kinetic energy Thus in the flow of the fluid mass there is also a flow of kinetic energy. The horizontal kinetic energy flow is $u(\rho E_{kx})$ and the vertical kinetic energy flow is $w(\rho E_{kz})$, where the kinetic energy on the horizontal axis is $E_{kx} = \frac{u^2}{2g}$ while the kinetic energy on the vertical axis is $E_{kz} = \frac{w^2}{2g}$, ρ is the mass density of water. To formulate the kinetic energy conservation equation, the control volume in Fig (2) is used.

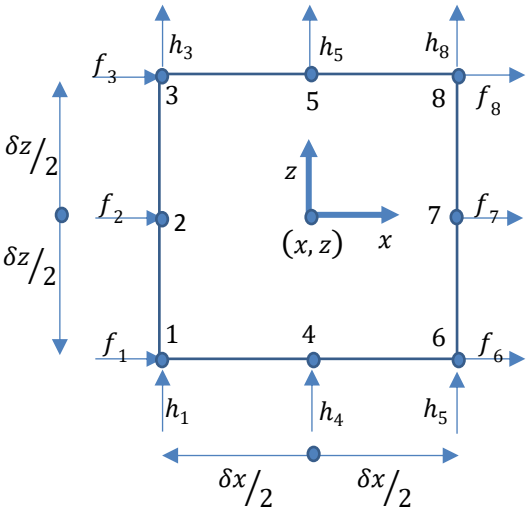

Fig (2). Control volume.

a. Space Averaging

The velocity distribution on the sides of the control volume is not uniform, so an average velocity that represents the flow velocity on each side is required.

Defined as

$f(x,z,t) = u(\rho E_{kx})$

$h(x,z,t) = w(\rho E_{kz})$

The horizontal kinetic energy input to the control volume through side $\overline{123}$ at a time $t = t$, is

$$f_1 = f\left(x - \frac{\delta x}{2}, z - \frac{\delta z}{2}, t\right) = f(x,z,t) - \gamma_x \frac{\delta x}{2}\frac{\partial f}{\partial x} - \gamma_z \frac{\delta z}{2}\frac{\partial f}{\partial z}$$

$$f_2 = f\left(x - \frac{\delta x}{2}, z, t\right) = f(x,z,t) - \gamma_x \frac{\delta x}{2}\frac{\partial f}{\partial x}$$

$$f_3 = f\left(x - \frac{\delta x}{2}, z + \frac{\delta z}{2}, t\right) = f(x,z,t) - \gamma_x \frac{\delta x}{2}\frac{\partial f}{\partial x} + \gamma_z \frac{\delta z}{2}\frac{\partial f}{\partial z}$$

The kinetic energy input rate on the $\overline{123}$ side is defined as

$$f_{input} = \frac{f_1 + f_2 + f_3}{3}$$

Substitution of the equations of f_1, f_2 and f_3 obtained

$$f_{input} = f_2 = f\left(x - \frac{\delta x}{2}, z, t\right) = f(x,z,t) - \gamma_x \frac{\delta x}{2}\frac{\partial f}{\partial x}$$

Using the same method, the following was obtained

$$f_{output} = f_7 = f\left(x + \frac{\delta x}{2}, z, t\right) = f(x,z,t) + \gamma_x \frac{\delta x}{2}\frac{\partial f}{\partial x}$$

$$h_{input} = h_4 = h\left(x, z - \frac{\delta z}{2}, t\right) = h(x,z,t) - \gamma_z \frac{\delta z}{2}\frac{\partial h}{\partial z}$$
$$h_{output} = h_5 = h\left(x, z + \frac{\delta z}{2}, t\right) = h(x,z,t) + \gamma_z \frac{\delta z}{2}\frac{\partial h}{\partial z}$$

b. Time averaging

The inflow and outflow of kinetic energy is observed at a very small time interval δt. At that time interval, although very small, there is certainly a change in velocity. Therefore, an average velocity that represents the velocity at the time interval δt is required. Defined the average velocity at the time interval from $t = -\frac{\delta t}{2}$ ke $t = \frac{\delta t}{2}$ is,

$$\bar{f_t} = \frac{f\left(x,z,t-\frac{\delta t}{2}\right) + f(x,z,t) + f\left(x,z,t+\frac{\delta t}{2}\right)}{3}$$

Using the weighted Taylor series, the following was obtained

$f_t = f(x,z,t)$

Thus, for the inflow outflow process at an interval of δt, the velocity at time $t = t$ can be used.

The kinetic energy inflow-outflow at time interval δt is

$IO = (f_{input} - f_{output})\delta z\, \delta t + (h_{input} - h_{output})\delta x\, \delta t$

By working out the input and output equations on the sides of the control volume that has been formulated, the followings are obtained

$$IO = \left(-\gamma_x \delta x \frac{\partial f}{\partial x}\right)\delta z \delta t + \left(-\gamma_z \frac{\partial h}{\partial z}\right)\delta x \delta t$$

The inflow-outflow causes a change in kinetic energy in the control volume,

$\delta E_k = (\delta E_{kx} + \delta E_{kz})\rho \delta x \delta z$

The principle of conservation of energy,

$$(\delta E_{kx} + \delta E_{kz})\rho \delta x \delta z = \left(-\gamma_x \delta x \frac{\partial f}{\partial x}\right)\delta z \delta t + \left(-\gamma_z \frac{\partial h}{\partial z}\right)\delta x \delta t$$

The substitute the definition of f and h and work on the assumption of incompressible flow are

$$(\delta E_{kx} + \delta E_{kz})\rho \delta x \delta z = \left(-\gamma_x \delta x \rho \frac{\partial u E_{kx}}{\partial x}\right)\delta z \delta t + \left(-\gamma_z \rho \frac{\partial w \rho E_{kz}}{\partial z}\right)\delta x \delta t$$

Both parts of the equation are divided by $\rho \delta x \delta z \delta t$, and worked out at very small δt close to zero,

$$\frac{\partial E_{kx}}{\partial t} + \frac{\partial E_{kz}}{\partial t} = -\gamma_x \frac{\partial u E_{kx}}{\partial x} - \gamma_z \frac{\partial w E_{kz}}{\partial z} \quad \text{.....(10)}$$

This equation is the kinetic energy conservation equation.

4.3. Euler's momentum conservation equation in horizontal direction.

By using the weighted Taylor series and by using the same fluid flow conditions as the continuity equation formulation where horizontal velocity only changes in the horizontal axis and vertical velocity only changes in the vertical axis, Hutahaean (2024a) obtained Euler's momentum conservation equation in the horizontal direction is,

$$\gamma_{t,3}\frac{\partial u}{\partial t} + \frac{\gamma_x}{2}\frac{\partial uu}{\partial x} = -\gamma_{t,3}\frac{\partial}{\partial x}\int_z^\eta \frac{\partial w}{\partial t}dz - \frac{\gamma_z}{2}\frac{\partial}{\partial x}\left(w_\eta w_\eta - ww\right) - g\frac{\partial \eta}{\partial x} \quad \text{.....(11)}$$

V. VERTICAL WATER PARTICLE VELOCITY EQUATION.

Vertical water particle velocity equation is formulated by integrating the continuity equation with respect to water depth.

$$\gamma_x \int_{-h}^{\eta} \frac{\partial u}{\partial x}dz + \gamma_z w_\eta - \gamma_z w_{-h} = 0$$

This equation is written as an equation for w_η where the bottom vertical water particle velocity is ignored,

$$w_\eta = -\frac{\gamma_x}{\gamma_z}\int_{-h}^{\eta}\frac{\partial u}{\partial x}dz$$

Integration of the right-hand segment is solved by Leibniz Integration (Protter, Murray, Morrey, & Charles, 1985)

$$\int_\alpha^\beta \frac{\partial f}{\partial x}dz = \frac{\partial}{\partial x}\int_\alpha^\beta f\, dz - f_\beta \frac{\partial \beta}{\partial x} + f_\alpha \frac{\partial \alpha}{\partial x}$$
$$\int_{-h}^{\eta}\frac{\partial u}{\partial x}\, dz = \frac{\partial}{\partial x}\int_{-h}^{\eta} u\, dz - u_\eta \frac{\partial \eta}{\partial x} - u_{-h}\frac{\partial h}{\partial x}$$

The integration of the first term of the right segment is solved by the depth average velocity concept and the bottom horizontal water particle velocity is ignored and substituted into the vertical velocity equation,

$$w_\eta = -\frac{\gamma_x}{\gamma_z}\left(\beta_u \frac{\partial UD}{\partial x} - u_\eta \frac{\partial \eta}{\partial x}\right)$$

Transformation into depth average velocity equation,

$$W = -\frac{\gamma_x}{\alpha_{w\eta}\gamma_z}\left(\beta_u \frac{\partial UD}{\partial x} - \alpha_{u\eta} U \frac{\partial \eta}{\partial x}\right) \quad \text{.....(12)}$$

Where,

$D = h + \eta$ is the total water depth. The coefficient β_u, defined in Equation (5). The coefficient $\alpha_{w\eta}$ outlined in Equation (8), serves as the transformation coefficient from surface vertical water particle velocity to depth-averaged vertical water particle velocity. Similarly, $\alpha_{u\eta}$ specified in Equation (7) is the transformation coefficient from surface horizontal water particle velocity to depth-averaged horizontal water particle velocity.

VI. WATER SURFACE ELEVATION EQUATION.

Water surface elevation equation is formulated by using Kinematic Free Surface Boundary Condition and kinetic energy conservation equation.

6.1.Kinematic Free Surface Boundary Condition.

Weighted kinematic water particle velocity is

$$w_\eta = \gamma_{t,2}\frac{\partial \eta}{\partial t} + \gamma_x u_\eta \frac{\partial \eta}{\partial x}$$

Written as water surface elevation equation,

$$\frac{\partial \eta}{\partial t} = \frac{1}{\gamma_{t,2}}\left(w_\eta - \gamma_x u_\eta \frac{\partial \eta}{\partial x}\right)$$

Added with depth average velocity variable, the water surface elevation equation becomes,

$$\frac{\partial \eta}{\partial t} = \frac{1}{\gamma_{t,2}}\left(\alpha_{w\eta} W - \gamma_x\, \alpha_{u\eta} U \frac{\partial \eta}{\partial x}\right) \quad \ldots\ldots(13)$$

6.2. Integration of the conservation of energy equation.

The energy conservation equation is multiplied by dz and integrated over the water depth,

$$\frac{1}{2g}\left(\int_{-h}^{\eta}\frac{\partial uu}{\partial t}dz + \int_{-h}^{\eta}\frac{\partial ww}{\partial t}dz\right) = \frac{1}{2g}\left(-\gamma_x\int_{-h}^{\eta}\frac{\partial uuu}{\partial x}dz - \gamma_z\left(w_\eta^3 - w_{-h}^3\right)\right)$$

Although there is an element of $\frac{1}{2g}$, in both segments of the equation, it cannot be removed, this is to keep the unit of the equation the same as the unit of the Kinematic Free Surface Boundary Condition, which is m/sec.

The integration is solved by Leibniz integration method and by working on the concept of depth average velocity and bottom water particle velocity is ignored,

$$\lambda\frac{\partial \eta}{\partial t} = \frac{1}{2g}\left(-\frac{\partial UU}{\partial t} - \frac{\beta_w}{\beta_u}\frac{\partial WW}{\partial t} - \frac{\gamma_x}{\beta_u D}\left(\beta_u\frac{\partial U^3 D}{\partial x} - \alpha_{u\eta}U^3\frac{\partial \eta}{\partial x}\right) - \frac{\gamma_z\alpha_{w\eta}}{\beta_u D}W^3\right)$$

Where,

$$\lambda == \frac{\left(\left(\beta_u - \alpha_{u\eta}\right)\frac{UU}{2g} + \left(\beta_w - \alpha_{w\eta}\right)\frac{WW}{2g}\right)}{\beta_u D}$$

The water surface change equation is the sum of the water surface change from the Kinematic Free Surface Boundary Condition and the water surface elevation equation change from the energy conservation equation.

$$(1+\lambda)\frac{\partial \eta}{\partial t} = \frac{1}{\gamma_{t,2}}\left(\alpha_{w\eta} W - \gamma_x\, \alpha_{u\eta} U \frac{\partial \eta}{\partial x}\right) - \frac{1}{2g}\left(\frac{\partial UU}{\partial t} + \frac{\beta_w}{\beta_u}\frac{\partial WW}{\partial t} + \frac{\gamma_x}{\beta_u D}\left(\beta_u\frac{\partial U^3 D}{\partial x} - \alpha_{u\eta}U^3\frac{\partial \eta}{\partial x}\right) + \frac{\gamma_z\alpha_{w\eta}}{\beta_u D}W^3\right) \quad \ldots.(14)$$

Equation (14) is the final water surface elevation equation of the water surface elevation equation. In the right segment of the equation there is a change in kinetic energy which is the source of energy for the change in potential energy in the left segment, Thus this equation can be called the energy conservation equation, which is a balance equation between changes in potential energy and changes in kinetic energy.

VII. HORIZONTAL WATER PARTICLE VELOCITY EQUATION.

Equation (11) is worked out on the surface at $z = \eta$,

$$\gamma_{t,3}\frac{\partial u_\eta}{\partial t} + \frac{\gamma_x}{2}\frac{\partial u_\eta u_\eta}{\partial x} = -g\frac{\partial \eta}{\partial x}$$

By using variable depth average velocity,

$$\gamma_{t,3}\alpha_{u\eta}\frac{\partial U}{\partial t} + \frac{\gamma_x\alpha_{u\eta}}{2}\frac{\partial UU}{\partial x} = -g\frac{\partial \eta}{\partial x} \quad \ldots.(15)$$

VIII. NUMERICAL METHOD

The space differential is solved by the Finite Difference Method while the time differential is solved by the predictor-corrector method. Details of the numerical methods as used by Hutahaean (2024a).

IX. MODEL OUTCOME

a. Wilson's Criteria (1963)

Wilson (1963) categorized wave profiles based on the ratio of wave crest elevation to wave height (Fig (3)). The wave profiles based on the comparison numbers are presented in Table (3).

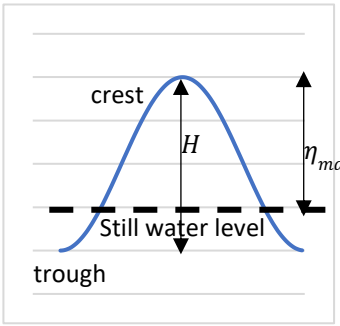

Fig (3). Water wave profile according to Wilson (1963).

Table (3) Water wave profile criteria (Wilson (1963))

Wave type	$\frac{\eta_{max}}{H}$
Airy/sinusoidal waves	< 0.505
Stoke's waves	$0.505 - 0.635$
Cnoidal waves	$0.635 - 1$
Solitary waves	$= 1$

a. Model execution at constant water depth..

In this section, the results of model execution at constant water depth (Fig (4)) are presented, with two water depths, $h = 20.0$ and $h = 8.0$ m.

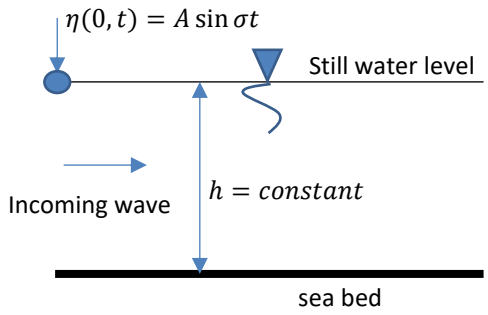

Fig (4). Constant water depth

As input, sinusoidal waves with the equation $\eta(0,t) = A \sin \sigma t$, is used, where $\sigma = \frac{2\pi}{T}$, T is the wave period, $T = 8.0$ sec. While wave amplitude A is used from 0.3-1.3 m, in order to obtain the types of wave profiles at various wave amplitudes.

a.1. Wave amplitude $A = 0.30$ m
The model execution results at $h = 20.0$ m is shown in Fig (5), where $\frac{\eta_{max}}{H} = \frac{0.33}{0.6} = 0.55$, is quite close to Wilson's sinusoidal profile criteria. The model execution results at $h = 8.0$ m is presented in Fig (6), where $\frac{\eta_{max}}{H} = \frac{0.37}{0.6} = 0.62$, which according to Wilson's criteria belongs to Stoke's profile.

On Stoke's profile, there is a deflection at the transition from wave crest to wave trough at $\eta \approx 0.0\,m$. The deflection can be the difference between sinusoidal profile and Stoke's profile. In the sinusoidal profile Fig (5), the deflection is actually visible but still very weak, the deflection can be eliminated by reducing the wave amplitude, thereby at deep water depth $h = 20.0$ m, wave amplitude $A = 0.30$ m is the transition limit from sinusoidal profile to Stoke's profile.

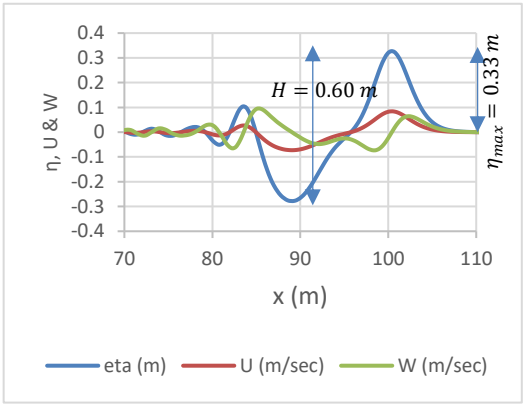

Fig (5). Sinusoidal wave profile, $A = 0.30\,m$, $h = 20.0\,m$

a.2. Wave amplitude $A = 0.60$ m
The model execution results at $h = 20.0$ m are presented in Fig (7), where $\frac{\eta_{max}}{H} = \frac{0.70}{1.2} = 0.583$, which based on Wilson's criteria belongs to Stoke's profile. In addition, there is a deflection at the transition from wave crest to wave trough, this deflection is also found in the Stoke's profile in Fig. (6). Fig (8) presents the model execution results at water depth $h = 8.0$ m, where $\frac{\eta_{max}}{H} = \frac{0.87}{1.2} = 0.725$, with the wave profile belonging to the cnoidal profile. Deflection changes to a small wave crest.

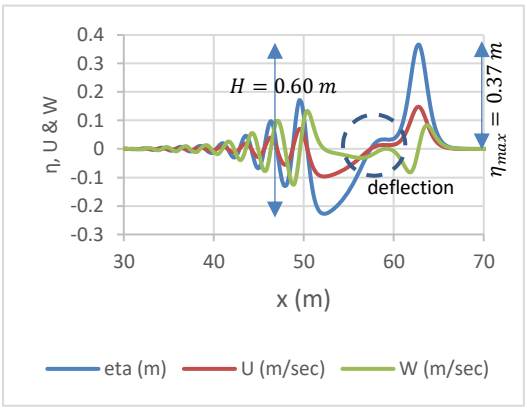

Fig (6). Stoke's wave profile, $A = 0.30\,m$, $h = 8.0\,m$

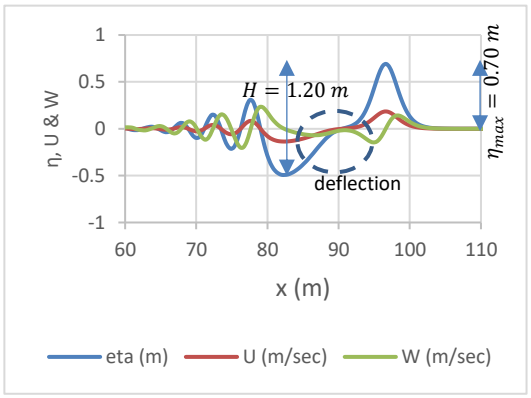

Fig (7). Stoke wave profile, $A = 0.60\,m$, $h = 20.0\,m$

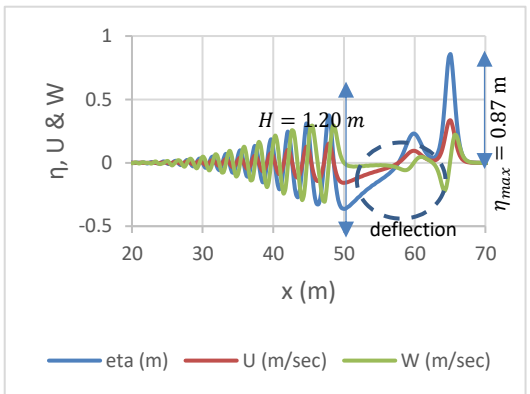

Fig (8). Cnoidal wave profile, $A = 0.60\,m$,

$h = 8.0\ m$

a.2. Wave amplitude $A = 1.30$ m

The model execution results at $h = 20.0$ m are shown in Fig (9), where $\frac{\eta_{max}}{H} = \frac{1.75}{2.5} = 0.7$ which according to Wilson's criteria belongs to the Cnoidal profile. The wave height is reduced from $H = 2.60\ m$ to $2.50\ m$, that is assumed due to deflection in the form of small wave. In Fig (10), the model execution results at water depth $h = 8.0\ m$ are presented, three wave crests are formed, the largest of which is the main wave. In this case, the main wave can be classified as a solitary wave with wave height $H = 2.20\ m$, considering that the entire wave body is above the still water level. There is a reduction in wave height because some of the wave energy is used to form two small waves, one of which has a solitary wave profile.

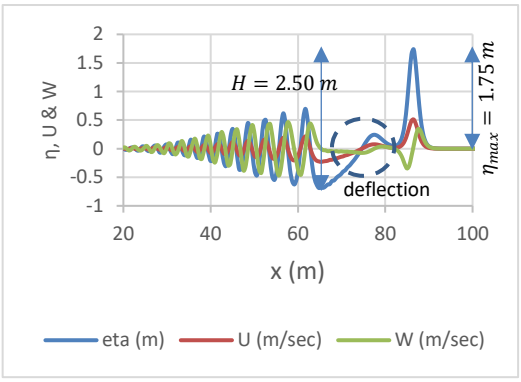

Fig (9). Cnoidal wave profile, $A = 1.30\ m$, $h = 20.0\ m$

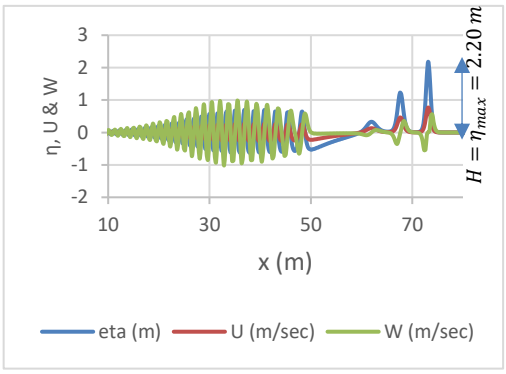

Fig (10). Solitary wave profile, $A = 1.30\ m$, $h = 8.0\ m$

The results from the model execution at a constant water depth revealed that sinusoidal wave profiles typically manifest in waves with small amplitudes. The formation of a wave profile is influenced by both the wave amplitude and the water depth. In deep water, a wave with a given amplitude might exhibit a sinusoidal profile, whereas the same amplitude in shallow water could result in a Stoke's profile. Conversely, a Stoke's profile in deep water may transition into a cnoidal profile in shallow waters, and a cnoidal profile in deep water can evolve into a solitary profile when the water depth decreases.

The distinction between a sinusoidal profile and a Stoke's profile is not only evident through the Wilson criteria but also by the characteristic deflection seen in the Stoke's profile, which appears as a flattened line at the transition from wave crest to wave trough. In contrast, in a cnoidal profile, this deflection manifests as small, gently sloping waves, and in a solitary profile, the deflection presents as two or more smaller waves.

Additionally, the primary wave is often accompanied by a tail wave or multiple secondary waves. The phenomena of shoaling and breaking of these secondary waves, which will be further discussed in the following section, are critical aspects of coastal wave dynamics.

b. Model execution at sloping bottom.

In this section, the model is executed on a sloping sea bed (Fig (11)), with water depth 15.0-1.0 m, bottom slope $\frac{14.0}{150.0} = 0.093$.

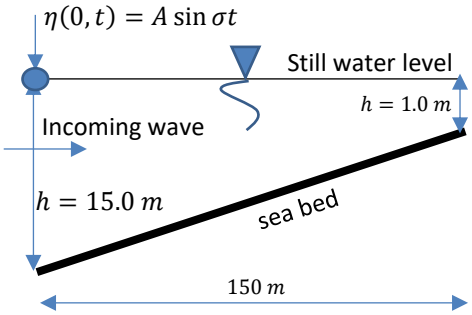

Fig (11). Sloping sea bed

In the simulation, a wave with a period of 8 seconds and an amplitude of 1.00 meter was input. Unlike previous depictions, the simulation results for this sloping bottom scenario are presented with the water depth h on the abscissa, allowing for a clear visualization of the relationship between water depth and wave characteristics. The waves transition from deep to shallow water, indicating that in the model, waves move from right to left.

The simulation was conducted until the main wave reached a water depth of approximately ≈ 1.3 m. The results are presented in Figure (12) and Figure (13). At this depth $h \approx 1.3\ m$, the height of the main wave stabilizes at 0.6 meters, and the wave profile transitions to a solitary profile, as shown in Figure (13).

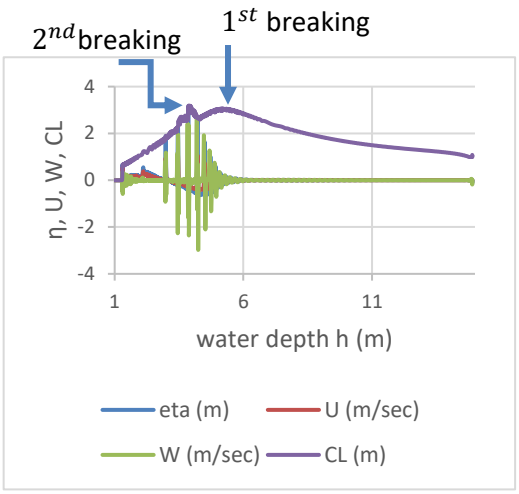

Fig (12). Wave condition after breaking.

Notes: CL (Crest Line) is the line that connects the maximum water level elevation along the wave trajectory. In Figure 12, it is apparent that there are two breaking events; however, there are actually more than two, as will be demonstrated in the next section (Figure 14). The first breaking event, which occurs at greater water depths, involves the main wave, while the second event, occurring in shallower waters, involves the breaking of the tail wave or secondary wave.

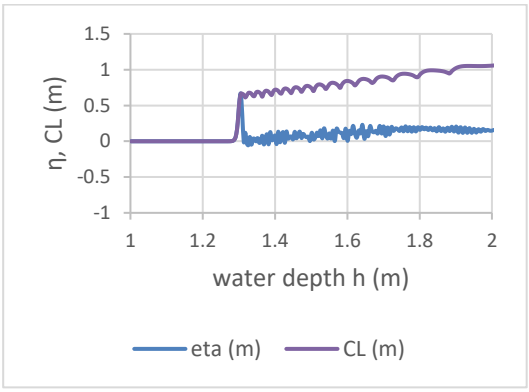

Fig (13). Main wave profile at water depth ≈ 1.3 m

The wave condition after the first breaking in the surf zone is highly unstable, as observed in the unstable crest line (Fig. (13) and Fig. (14)). Wave instability in the surf zone is a well-documented phenomenon. Within this zone, the secondary wave experiences breaking, which is depicted in Fig.(14), where two breakings occur in two secondary waves. The wave profile is a solitary profile, as shown in Fig.(15).

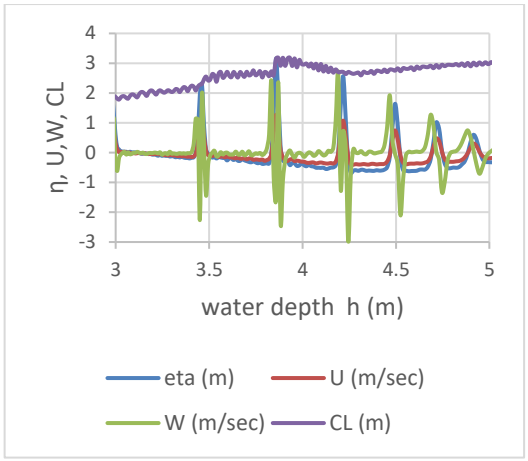

Fig (14). Breaking of the secondary wave.

There are 3 breaking points with 3 breaking conditions, namely :

a. Main wave breaking, $H_{br} = 3.06$ m ,
$h_{br} = 5.17$ m, $\frac{H_{br}}{h_{br}} = 0.59$

b. 1st secondary wave breaking 1 $H_{br} = 3.19$ m,
$h_{br} = 3.87$ m, $\frac{H_{br}}{h_{br}} = 0.82$

c.2nd secondary wave breaking $H_{br} = 2.3$ m ,
$h_{br} = 3.45$ m, $\frac{H_{br}}{h_{br}} = 0.67$

Breaker height as suggested by Komar and Gaughan (1972) is:

$$H_{br} = 0.39\, g^{1/5}(T_0 H_0^2)^{2/5} \quad \text{.....(16)}$$

Where $T_0 = 8.0$ sec., $H_0 = 2.00$ m, $g = 9.81$ m/sec^2 obtain $H_{br} = 2.46$ m. The closest model result is the 2nd secondary breaking wave $H_{br} = 2.2$ m.

Breaker depth index from Mc Cowan (1894),

$$\frac{H_{br}}{h_{br}} = 0.78 \quad \text{.....(17)}$$

The closest model result is the breaking of the 1st secondary wave $\frac{H_{br}}{h_{br}} = 0.82$.

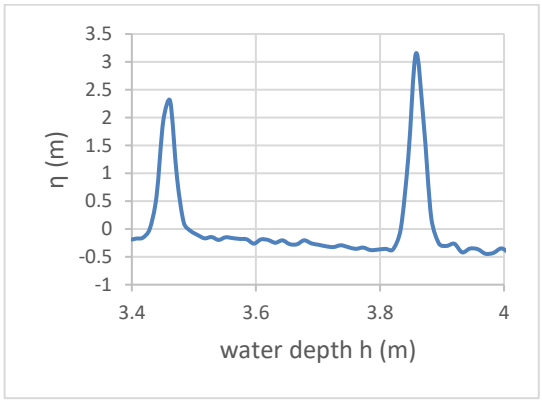

Fig (15). Breaking wave profile of the secondary wave.

Next, the breaking condition of the main wave is shown (Fig. (16)) with the wave profile being a solitary profile, Fig. (17).

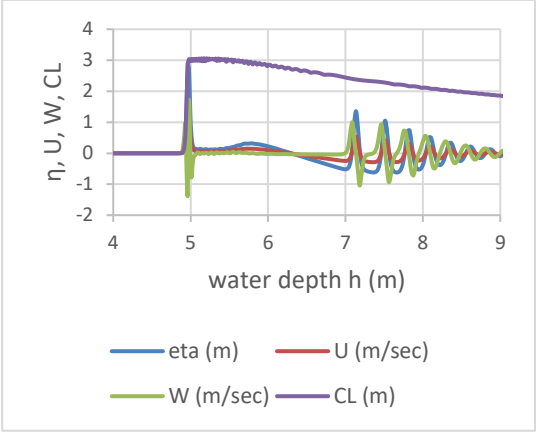

Fig (16). The breaking condition of the main wave.

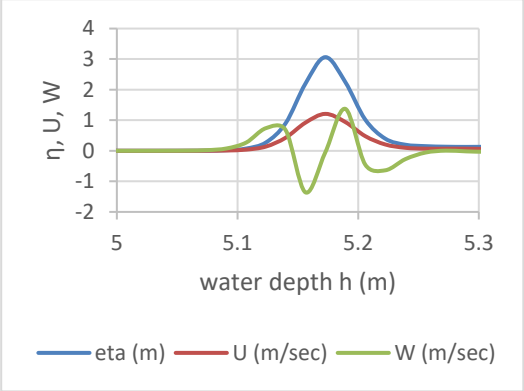

Fig (17). Wave profile of the main wave at the breaking point.

The model results from the sloped bottom indicate that it can effectively simulate the shoaling-breaking process and subsequent movement in very shallow water depths. The simulation identifies three types of breaking waves: a primary breaking wave and two secondary breaking waves, with the wave profile adopting a solitary shape at the moment of breaking. If the simulation continues, there may be additional breakings, such as a fourth and fifth wave.

Additionally, the model reveals a significant increase in vertical water particle velocity at the point of breaking. According to the continuity equation, a decrease in water depth leads to a greater disparity between input and output in the horizontal direction, which, in turn, escalates the vertical velocity. Thus, there is a likelihood that wave breaking may occur when the vertical velocity becomes excessively high.

X. CONCLUSION

The study demonstrated that by incorporating Surface Kinematic Boundary Conditions as the water surface elevation equation and combining it with the kinetic energy conservation equation, a model was developed capable of simulating wave breaking until a reduction in wave height occurs in shallow water. This combination generates an equation that adheres to the energy conservation principle, establishing a balance between potential energy changes, indicated by variations in water surface elevation, and kinetic energy changes.

The model, with modifications to its calculation algorithm, consistently generates four distinct wave profiles according to wave height and water depth: sinusoidal, Stoke's, cnoidal, and solitary profiles. Overall, the model effectively simulates water wave mechanics in both deep and shallow water environments.

Future developments should focus on refining the estimation of breaker height and depth to align more closely with the results obtained from physical model studies conducted by previous researchers, as well as those derived from velocity potential theory.

REFERENCES

[1] Hutahaean, S. (2024a). Applying Weighted Taylor Series on Time Series Water Wave Modeling. International Journal of Advance Engineering Research and Science (IJAERS). Vol. 11, Issue 2; Feb, 2024, pp 38-47. Article DOI: https://dx.doi..org/10.22161/ijaers.112.6.

[2] Boussinesq, J. (1871) Theorie de l'intumescence liquede,aplelee onde ou de translation, se propageant dans un canal rectangulaire. Comptes Rendus de l'Academic des Sciences. **72**:755-759.

[3] Dingermans, M.W. (1997). Wave propagation over uneven bottom. Advances series on Ocean Engineering **13.** World Scientific, Singapore. ISBN 978-981-02-0427-3. Archived from the original on 2012-0-08. Retrieved 2008-01-21, Chapter 5.

[4] Hamm, L.; Madsen, P.A.; Peregrine, D.A. (1993). Wave transformation in the nearshore zone: A Review. Coastal Engineering. **21** (1-3):5-39. Doi:10.1016/0378-3839(93)90044-9.

[5] Johnson, R.S. (1997). A modern introduction to the mathematical theory ofwater waves. Cambridge Texts in Applied Mathematics. **19.** Cambridge University Press ISBN 0 521 59832 X.

[6]Kirby, J.T. (2003). Boussinesq Models and Applications to nearshore wave propagation, surfzone process and waves induced currents. In Lakhan, V.C. (ed). Advances in Coastal Modeling. Elsevier Oceanography Series.**67.** Elsevier, pp. 1-41. ISBN 0 444 51149 0.

[7] Peregrine, D.H. (1967). Long waves on a Beache. Journal of Fluid Mechanics. **27** (4): 815-824. Bibcode: 1967 JFM.....815P. doi:10.1017/S0022112067002605.

[8] Peregrine, D.H. (1972). Equations for water waves and the propagation approximations behind them. In Meyer, R.E.(ed). Wave on Beaches and Resulting Sediment Transport. Academic Press.pp.95-122. ISBN 0 12 493 250 9.

[9] Hutahaean, S., Achiari H. (2017). Non-Linear Water Wave Equation Time Series Formulated Using Velocity Equation as The Result of Laplace Equation. International Journal of Engineering Research and Application (IJERA). Vol. 7, Issue 6, Part (-3); June, 2017, pp 37-45.

[10] Hutahaean, S. (2019). A Continuity Equation For Time Series Water Wave Modeling Formulated Using Weighted Total Acceleration. International Journal of Advance Engineering Research and Science (IJAERS). Vol. 6, Issue 9; Sept, 2019, pp 148-153. Article DOI: https://dx.doi..org/10.22161/ijaers.69.16.

[11] Hutahaean, S. (2024b). Breaking Index Study on Weighted Laplace Equation. International Journal of Advance Engineering Research and Science (IJAERS). Vol. 11, Issue 1; Jan, 2024, pp 34-43. Article DOI: https://dx.doi..org/10.22161/ijaers.11.6.

[12] Hutahaean, S. (2023). Method for Determining Weighting Coefficients in Weighted Taylor Series Applied to Water Wave Modeling. International Journal of Advance Engineering Research and Science (IJAERS). Vol. 10, Issue 12; Dec, 2023, pp 105-114. Article DOI: https://dx.doi..org/10.22161/ijaers.1012.11.

[13] Dean, R.G., Dalrymple, R.A. (1991). Water wave mechanics for engineers and scientists. Advance Series on Ocean Engineering.2. Singapore: World Scientific. ISBN 978-981-02-0420-4. OCLC 22907242.

[14] Protter, Murray, H.; Morrey, Charles, B. Jr. (1985). Differentiation Under The Integral Sign. Intermediate Calculus (second ed.). New York: Springer pp. 421-426. ISBN 978-0-387-96058-6.

[15] Wilson, B.W. (1963). Condition of Existence for Types of Tsunami Waves, paper presented at XIIIth Assembly IUGG, Berkeley, California, August 1963 (unpublish).

[16] Komar, P.D. & Gaughan M.K. (1972). Airy Wave Theory and Breaker Height Prediction, Coastal Engineering Proceedings, 1 (13).

[17] Mc Cowan, J. (1894). On the highest waves of a permanent type, Philosophical Magazine, Edinburgh 38, 5th Series, pp. 351-358.